

Quantifying Anthropomorphism of Robot Arms

Christoforos I. Mavrogiannis, Minas V. Liarokapis and Kostas J. Kyriakopoulos

Abstract—In this paper we introduce an index for the quantification of anthropomorphism of robot arms. The index is defined as a weighted sum of specific metrics which evaluate the similarities between the human and robot arm workspaces, providing a normalized score between 0 (non-anthropomorphic artifacts) and 1 (human-identical artifacts). The human arm workspaces were extracted using data reported in anthropometry studies. The formulation is general enough to allow utilization in various applications, by adjusting the weighting factors according to the specifications of each study. The proposed methodology can be used for assessing the human-likeness of existing robot arms as well as to provide specifications for the design of new anthropomorphic robots and prosthetic devices. To assess the efficiency of the proposed methods a comparative analysis between five kinematically different robot arm models is conducted and simulated paradigms are presented.

Index Terms: Anthropomorphism, Robot Arms Design, Human Robot Interaction.

I. INTRODUCTION

Anthropomorphism, as described in [1], is the tendency to imbue the imagined or real behavior of nonhuman agents with human-like characteristics, motivations, intentions and emotions. The word anthropomorphism originates from the Greek words *anthropos* and *morphe*, meaning *human* and *form* respectively. According to [2], we can identify at least two dimensions of similarity between humans and robots: similarity in terms of motion and similarity in terms of morphology. Similarity in motion depends on the kinematic model (relative link lengths and joint positions) and the joint coordination patterns (encapsulated in the concept of synergies from neuroscience). Similarity in morphology concerns the degree of correspondence for visually perceived characteristics such as shape and size for robotic artifacts or even facial expressions for humanoid robots.

Christoforos I. Mavrogiannis is with the Sibley School of Mechanical & Aerospace Engineering, Cornell University, Upson Hall, 124 Hoy Road, Ithaca, NY 14853, USA. Email: cm694@cornell.edu

Minas V. Liarokapis is with the Department of Mechanical Engineering and Materials Science, Yale University, Mason Laboratory, 9 Hillhouse Avenue, New Haven, CT 06520, USA. Email: minas.liarokapis@yale.edu

Kostas J. Kyriakopoulos is with the Control Systems Lab, School of Mechanical Engineering, National Technical University of Athens, 9 Heron Polytechniou Str, Athens, 15780, Greece. Email: kkyria@mail.ntua.gr

This work has been partially supported by the European Commission with the Integrated Project no. 248587, THE Hand Embodied, within the FP7-ICT-2009-4-2-1 program Cognitive Systems and Robotics.

Nowadays anthropomorphism is becoming increasingly important for robotics applications for two main reasons: 1) it ensures likeability of robotic artifacts and 2) it guarantees safety in Human Robot Interaction (HRI) applications. Humans are starting to interact and co-exist with robots in everyday life environments. Thus, the more humanlike a robot is in terms of appearance, perceived intelligence and motion the more easily it will manage to establish solid social connections with humans.

Nevertheless, anthropomorphism can also improve safety and efficiency of HRI applications as human-like motion can be intuitively understood by humans. More specifically, anthropomorphism may increase a robot's capability for motion expressiveness, which can be critical in scenarios where robots have to cooperate closely with humans to accomplish a task. In this respect, anthropomorphic arms can generate predictable motion, avoiding to surprise or confuse their human partner, or even generate suboptimal legible motion that is more intent expressive, thus leading to increased overall safety and efficiency [3].

The problem of quantifying anthropomorphism of robotic artifacts has been addressed lately, with most studies focusing on the human-likeness of robot hands. In [4] and [5] an index of anthropomorphism was proposed that is defined as a weighted sum of scoring functions related to kinematics, contact surfaces and size. In [6], the authors performed a review of performance characteristics for prosthetic and anthropomorphic robot hands. The review was based on a qualitative analysis and mainly focused on the mechanical characteristics of various hands. In [7] and [8], quantitative studies were conducted, using Gaussian Process - Latent Variable Models (GP-LVM) to represent the human and robot fingertip workspaces in low-dimensional manifolds. A comparison was then performed between the computed workspaces. In [9] the authors proposed a methodology for quantifying the functional workspace of the precision thumb - finger grasp, defined as the range of all possible positions in which thumb fingertip and each other fingertip, can simultaneously contact each other.

Recently, we proposed a methodology for quantifying the anthropomorphism of robot hands motion [10]. In this study, we proposed a series of metrics for assessing the relative coverages of human and robot finger phalanges workspaces, as well as human and robot fingers base frames workspaces. The total score of anthropomorphism for each hand was defined as a weighted sum of the aforementioned metrics. In this latter study three robot hands were examined and simulated workspace comparisons were presented.

Regarding arm workspace analyses, in [11] the authors presented a framework for representing the robot arm capabilities within different regions of its workspace as directional structures. Moreover, in [12], they used a reachability map to perform a comparison between a haptic interface and the reachable workspace of the human arm. The analysis focused on the position of the tool center point (TCP) of the robot arm in 3D space. For doing so, the reachable and dexterous workspaces of the robot arm were computed, following the directions provided in [13]. However, this study does not focus on examining the humanlikeness of robot arms' workspaces and does not take into account the human to robot link-to-link comparisons, that we argue to be necessary for the quantification of anthropomorphism.

In this paper we follow a similar approach with the one described in [10] in order to quantify the anthropomorphism of robot arms. Based on data provided by recent anthropometry studies [14], we compare human and robot arm workspaces in three different levels: 1) upper arm link workspaces, 2) forearm link workspaces and 3) wrist/hand link workspaces. Then we derive a similarity score for each level. The final score of anthropomorphism is defined as the linear combination of the aforementioned scores and ranges between 0 (non-anthropomorphic artifacts) and 1 (human-identical artifacts). A set of weights accounts for ranking subscores in terms of relative importance. The weights can be adjusted subjectively, according to the specifications and the goals of the study to be conducted. In order to validate the efficiency of the proposed methodology we perform a comparative analysis between four real robot arms and a hypothetical robot arm with total size equal to 110% of the mean human arm size. To the best of our knowledge, this is the first work that focuses on the quantification of anthropomorphism of robot arms.

The rest of the document is organized as follows: Section II focuses on the kinematic models and the apparatus used for our analysis, Section III describes the methods proposed to quantify anthropomorphism of robot arms, Section IV reports the results of the introduced metrics for a series of robot arms, while Section V concludes the paper.

II. KINEMATIC MODELS AND APPARATUS

A. Kinematic Model of the Human Arm

In order to make comparisons between human and robot arms, we need a human arm reference. In this paper we use the parametric model of the human arm, derived from anthropometry studies [15] to define the lengths of the human upper arm, forearm and wrist/hand links. The aforementioned model is defined parametrically with respect to (wrt) the human height. In this study we set the human height to be equal to the average height of the men and women 50th percentiles. This latter choice is based on data provided in [14], where the mean values for men and women USA citizens of age 20 years old and older, are presented.

It should be noted that the human height is a body parameter that varies significantly among different countries and ethnicity groups. For this reason, besides assessing the

anthropomorphism of robot arms by comparing them with the “mean” human arm, we are also computing normalized anthropomorphism scores, based on the normalized link lengths¹ to balance the bias introduced by the mean height assumption. To justify this choice, one might consider extreme examples: e.g., the arms of a little girl and a basketball player are both anthropomorphic, but when we compare their actual workspaces with the average human workspaces, they may be incorrectly classified as non-humanlike.

The human arm kinematics can be described with a model (see [16]) consisting of: three degrees of freedom (DoF) to model the shoulder joint (one for abduction/adduction, one for flexion/extension and one for internal/external rotation), two DoF for the elbow joint (one for flexion/extension and one for pronation/supination) and two DoF for the wrist (one for flexion/extension and one for abduction/adduction). The ranges of motion for each DoF were extracted from [17].

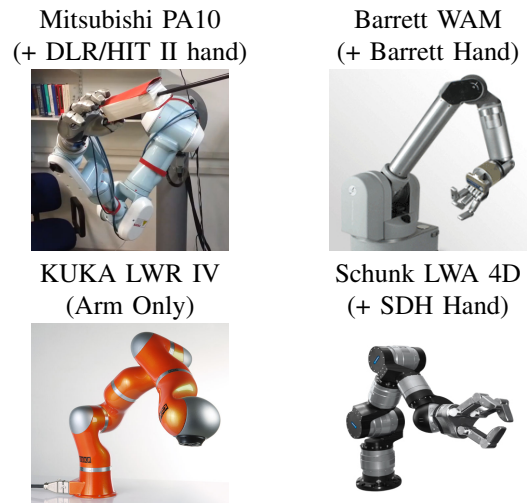


Fig. 1. The robot arms examined in this study.

B. Robot Arms

In this study, we assess the anthropomorphism of four existing robot arms and a hypothetical robot arm. The existing robot arms considered are: the 7 DoF Mitsubishi PA10 (Mitsubishi Heavy Industries) [18], the 7 DoF Barrett WAM (Barrett Technology Inc.) [19], the 7 DoF KUKA LWR 4 (KUKA Roboter GmbH) [20] and the 7 DoF Schunk LWA 4D (Schunk GmbH & Co) [21]. The robot arms are depicted in Fig. 1. The hypothetical robot arm has the same kinematic model with the human arm and total length equal to 110% of the human arm.

Remark 1: It should be noted that since the adopted human arm kinematic model is based on parametric models, then in order to scale the total length of the arm we just have to scale the height parameter, scaling also equivalently all the links lengths of the hypothetical robot (by 110%).

¹For each link, the normalized link length is defined as the ratio between the link length and the total arm length.

The human arm hand system is a highly sophisticated and dexterous mechanism, due to the complex kinematics of the human hand and the human shoulder. In this study, we consider each human and robot arm as a typical arm with three links: 1) the upper arm, 2) the forearm and 3) the wrist/hand, considering the hand as the end-effector. This choice is justified by the fact that the two DoF of the wrist are used to change the position and orientation of the hand, contributing significantly to its dexterity. It should be noted that some of the robot arms examined in this paper, do not have a third link. For example, the Schunk LWA 4D, the KUKA LWR IV and of course the hypothetical robot, only have two links. In order to be able to perform comparisons we attach the same hypothetical robot hand at the end-effectors of all robot arms, creating a third link or a third link offset with a size equal to the mean human hand size.

III. METHODS

A. Convex Hulls

The convex hull of a set of points S can be geometrically described as the intersection of all convex sets containing S . The convex hull of a finite point set S forms a convex polytope in \mathbb{R}^n . There are plenty of methods available to compute the convex hull of a set S of points. In this study we choose to use the well known quickhull algorithm for convex hulls, that was described in [22]. For more details regarding the decompositions of the convex hulls and their volumes, the reader may consult [23] and [24].

B. Creating Virtual Links for Robot Arms with m -Links

In case that a robot arm has more than three links we keep some DoF fixed in order to create virtual links corresponding to the humanlike grouping convention of the upper arm, forearm and wrist / hand links, that we adopt in this paper. More specifically, we are seeking link groupings that minimize the sum of the “distances” between the normalized robot and human link lengths:

$$d = \left| \frac{u_H}{t_H} - \frac{u_R}{t_R} \right| + \left| \frac{f_H}{t_H} - \frac{f_R}{t_R} \right| + \left| \frac{h_H}{t_H} - \frac{h_R}{t_R} \right| \quad (1)$$

where t_H is the total length of the human arm (sum of link lengths), t_R is the total length of the robot arm, u_H is the length of the human’s upper arm link, u_R is the length of the robot’s upper arm link, f_H is the length of the human’s forearm link, f_R is the length of the robot’s forearm link, h_H is the length of the human’s hand link and h_R is the length of the robot’s hand link. We generate all possible combinations of link groupings and we finally pick the one that minimizes the aforementioned cost d .

C. Workspace Computations

In order to assess anthropomorphism of robot arms, we perform one-to-one comparisons between polytopes defined by the workspaces of human and robot upper arm, forearm and wrist/hand links. For doing so, we first derive workspace representations, by generating corresponding sets of points. More specifically, for each link we discretize the range of

motion R for each of the k joints that are attached to it and contribute to its motion, choosing a step size of $\frac{R}{n}$, where n is the discretization variable². Then we explore the space of these joint angles while keeping the rest joints fixed at zero and we compute the forward kinematics for the active link and for all possible joint configurations $(n+1)^k$.

The generated sets are used to create the convex hulls to be compared. More specifically, for the upper arm we conclude to: 1) the set $S_U \subset \mathbb{R}^3$ that contains all the generated points of the upperarm workspace (all possible elbow joint positions) and the arm’s base position, 2) the set S_F that consists of all the generated points of the forearm workspace (all possible wrist joint positions) and the elbow joint position when the three first DoF are equal to zero and 3) the set S_H that contains all the points of the hand workspace (all possible hand positions) as well as the wrist position, when all DoF from 1 to 5 are fixed at zero. A convex hull is then computed for each of the extracted sets. Visualizations of the workspaces and the corresponding convex hulls of different links, are depicted in Fig. 2.

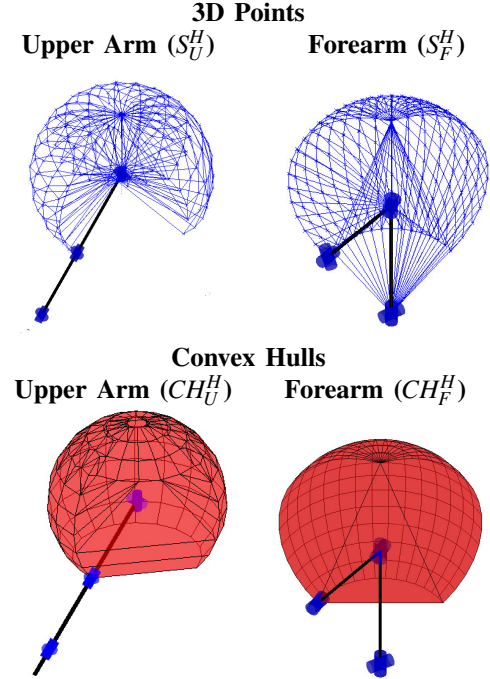


Fig. 2. Workspaces and the corresponding convex hulls for the upper arm and forearm links of the mean human arm.

D. Quantifying Anthropomorphism of Robot Arms with Actual Link Lengths

1) *Upper Arm Score*: Let S_U^H be the set of points of the human upper arm workspace (generated as described in the previous section) and S_U^R be the corresponding set of points of the robot upper arm workspace. We compute the corresponding convex hull for the human arm CH_U^H and for the robot arm CH_U^R . Let also $CH_U^I = CH_U^H \cap CH_U^R$ and

²_n Initially we used $n = 14$ for all joints, but then we varied the value to study its effect.

and $CH_U^U = CH_U^H \cup CH_U^R$ be respectively the intersection and union of the human and robot upper arm workspaces. The anthropomorphism score for the upper arm link of the robot arm (A_U), is defined as:

$$A_U = \frac{Vol(CH_U^I)}{Vol(CH_U^U)} 100(\%) \quad (2)$$

Remark 2: It should be noted that in order to not penalize the case that a robot arm is more dexterous than the human arm, if a robot arm has joints with ranges of motion greater than those of the equivalent joints of the human arm, we set them to be equal with the corresponding human limits.

2) *Forearm Score:* Following the same procedure as in the upper arm link case, we first define the human and robot sets of forearm workspace points S_F^H and S_F^R and we compute the corresponding convex hulls, CH_F^H and CH_F^R . Then we compute their intersection $CH_F^I = CH_F^H \cap CH_F^R$ and union $CH_F^U = CH_F^H \cup CH_F^R$. Thus, anthropomorphism for the forearm link of the robot arm (A_F), can be defined as:

$$A_F = \frac{Vol(CH_F^I)}{Vol(CH_F^U)} 100(\%) \quad (3)$$

3) *Hand Score:* Finally, for the hand case, we compute the human and robot sets of workspace points S_H^H , S_H^R and then the corresponding convex hulls CH_H^H and CH_H^R . Afterwards, we compute equivalently the intersection of human and robot workspaces $CH_H^I = CH_H^H \cap CH_H^R$, as well as their union $CH_H^U = CH_H^H \cup CH_H^R$ and we define the score of hand link anthropomorphism as:

$$A_H = \frac{Vol(CH_H^I)}{Vol(CH_H^U)} 100(\%) \quad (4)$$

4) *Total Score of Anthropomorphism for Robot Arms with Actual Link Lengths:* In order to compute the total score of anthropomorphism for each robot arm (A_R), we use a weighted sum of the computed scores for the robot upper arm, forearm and hand links, as follows:

$$A_R = \frac{w_U A_U + w_F A_F + w_H A_H}{w_U + w_F + w_H} (\%) \quad (5)$$

where $w_U, w_F, w_H \geq 0$ with $w_U + w_F + w_H = 1$, are respectively the weights of the scores of the upper arm, forearm and wrist/hand links and can be set subjectively according to the specifications of each study.

E. Quantifying Anthropomorphism of Robot Arms for Normalized Link Lengths

In order to quantify robot arms anthropomorphism without taking into account the total lengths of the human and robot arms, we also perform the aforementioned comparisons of the upperarm, forearm and wrist/hand link workspaces utilizing human and robot models with normalized link lengths. Thus, by employing the same equations (2-5), we compute the upper arm, forearm and hand anthropomorphism scores for the normalized link lengths A_U^N , A_F^N and A_H^N .

The score of anthropomorphism for the whole robot arm, for the case of normalized link lengths is then computed as:

$$A_R^N = \frac{w_U A_U^N + w_F A_F^N + w_H A_H^N}{w_U + w_F + w_H} (\%) \quad (6)$$

where w_U, w_F, w_H , are once again weights that adjust the relative importance of the anthropomorphism subscores with $w_U + w_F + w_H = 1, w_U, w_F, w_H > 0$.

IV. RESULTS AND SIMULATIONS

In this section, we present results extracted by computing the anthropomorphism scores for all considered robot arms, using as a reference the mean human arm, as described in the previous sections. The link workspaces were generated by setting $R/n = 14$ for all robot arm models. The total score for each robot arm was computed by considering all workspace similarity subscores to have the same importance, i.e., setting $w_U, w_F, w_H = \frac{1}{3}$. In order to compute the convex hulls, their unions and intersections and visualize the results we used the multiparametric toolbox (MPT) [25]. The simulated paradigms of the robot arms were generated using the Matlab Robotics Toolbox [26].

In Table I we present the anthropomorphism scores, for the case of the actual link lengths, for all link workspaces and for all considered robot models.

TABLE I
ANTHROPOMORPHISM SCORES FOR ROBOT ARMS WORKSPACES WITH ACTUAL LINK LENGTHS

Robot Arm	Upper Arm	Forearm	Wrist
Mitsubishi PA10	25.02%	11.69%	0%
Barrett WAM	23.76%	19.26%	0%
KUKA LWR IV	52.82%	19.43%	0%
Schunk LWA 4D	87.97%	64.82%	48.37%
HRobot	74.91%	71.92%	29.83%

In Table II, the scores of anthropomorphism for the arm models with normalized link lengths are presented. The comparison was done using the mean human arm with normalized link lengths. In Table III we present the average anthropomorphism scores for each link of each robot arm, defined as the mean value of the previous two anthropomorphism scores: 1) the score for the actual link lengths and 2) the score for the normalized link lengths. The total score of anthropomorphism for the case of the actual link lengths, can be found in Table IV. As it can be noticed, the Schunk LWA 4D and the Hypothetical robot arm, outperform the rest robot arms, in terms of humanlikeness.

TABLE II
ANTHROPOMORPHISM SCORES FOR ROBOT ARMS WORKSPACES WITH NORMALIZED LINK LENGTHS

RobotArm	Upper Arm	Forearm	Wrist
Mitsubishi PA10	39.31%	55.89%	66.01%
Barrett WAM	55.01%	56.47%	73.57%
KUKA LWR IV	80.08%	55.55%	44.86%
Schunk LWA 4D	93.81%	79.59%	84.95%
HRobot	100%	100%	100%

TABLE III
AVERAGE ANTHROPOMORPHISM SCORES FOR ROBOT ARMS
WORKSPACES

RobotArm	Upper Arm	Forearm	Wrist
Mitsubishi PA10	32.17%	33.79%	33.01%
Barrett WAM	39.39%	37.87%	36.79%
KUKA LWR IV	66.45%	37.49%	22.43%
Schunk LWA 4D	90.89%	72.21%	66.66%
HRobot	87.46%	85.96%	64.92%

TABLE IV
TOTAL SCORE OF ANTHROPOMORPHISM FOR ROBOT ARMS WITH
ACTUAL LINK LENGTHS.

Mitsubishi PA10	Barrett WAM	KUKA LWR	Schunk LWA	HRobot
14.68%	17.21%	28.90%	70.79%	64.70%

The total scores of anthropomorphism per robot, for the case of normalized link lengths, can be found in Table V. It is quite evident that for the normalized link lengths case, the scores of anthropomorphism are quite higher than in the case of the actual link lengths. Once again (as expected), the Schunk LWA 4D and the Hypothetical robot arm, outperform all other robot arms, being the most anthropomorphic.

TABLE V
TOTAL SCORE OF ANTHROPOMORPHISM FOR ROBOT ARMS WITH
NORMALIZED LINK LENGTHS.

Mitsubishi PA10	Barrett WAM	KUKA LWR	Schunk LWA	HRobot
51.28%	59.31%	63.22%	86.35%	100%

The average total score of anthropomorphism per robot, defined as the mean value of its total scores computed with actual and normalized link lengths, can be found in Table VI. These scores provide a balanced indicator of anthropomorphism for each arm since they take into account both the actual and the normalized link lengths scores.

TABLE VI
AVERAGE TOTAL SCORES OF ANTHROPOMORPHISM

Mitsubishi PA10	Barrett WAM	KUKA LWR	Schunk LWA	HRobot
32.98%	38.26%	46.06%	78.57%	82.35%

Finally, in Table VII, we present the effect of workspace sampling resolution (R/n) on the scores of anthropomorphism. We compute the scores of the upper arm anthropomorphism of the hypothetical arm by exploring the joint spaces with different sampling resolutions. As it can be noticed, the score differences become insignificant when $R/n > 9$. In this paper, we chose to use $R/n = 14$ since we observed that it offers fast convex hull computations and sufficient accuracy in the computations of the different scores of anthropomorphism.

In Fig. 3 we present visualizations of the convex hulls of the links workspaces for all considered robot arms, for the case of actual link lengths. The three capital Xs at the hand links of the Mitsubishi PA10, the KUKA LWR IV and

TABLE VII
EFFECT OF WORKSPACE RESOLUTION ON THE COMPUTATION OF THE
UPPER ARM SCORE OF ANTHROPOMORPHISM

R	R/7	R/8	R/9	R/10	R/14
Score	74.4955%	75.2556%	74.9189%	74.911481%	74.911480%

the Barrett WAM denote that no intersection between the human and the robot link workspaces was detected. Thus the “volume” of the intersection is zero and the corresponding anthropomorphism score also becomes zero, as reported in Table I. Finally, in Fig. 4 the convex hulls of the case of the normalized link lengths, are depicted.

V. CONCLUSIONS

In this paper we proposed a systematic approach to quantify the anthropomorphism of robot arms. A comparison was performed for five kinematically different robot arm models. The analysis was based on computational geometry and set theory methods. The proposed methodology can be used not only to assess the human-likeness of specific robot arms, but also to provide specifications for the design of the next generation of dexterous/anthropomorphic robot arms and upper limb prosthetic devices. Regarding future directions we plan to extend our analysis formulating a methodology for the quantification of anthropomorphism for complete robot arm hand systems as well as to assess anthropomorphism in non-kinematic domains (e.g., dynamic characteristics, stiffness etc.).

REFERENCES

- [1] N. Epley, A. Waytz, and J. Cacioppo, “On seeing human: A three-factor theory of anthropomorphism,” *Psychological Review*, vol. 114, no. 4, pp. 864–886, October 2007.
- [2] M. Liarokapis, P. Artemiadis, and K. Kyriakopoulos, “Functional anthropomorphism for human to robot motion mapping,” in *IEEE International Symposium on Robot and Human Interactive Communication (RoMan)*, sept. 2012, pp. 31–36.
- [3] A. D. Dragan and S. Srinivasa, “Integrating human observer inferences into robot motion planning,” *Auton. Robots*, vol. 37, no. 4, pp. 351–368, 2014.
- [4] L. Biagiotti, F. Lotti, C. Melchiorri, and G. Vassura, “How Far is the Human Hand? A Review on Anthropomorphic End Effectors,” DIES Internal Report, University of Bologna, Tech. Rep., 2004.
- [5] L. Biagiotti, “Advanced robotic hands: Design and control aspects,” Ph.D. dissertation, Università Degli Studi di Bologna, 2002.
- [6] J. Belter and A. Dollar, “Performance characteristics of anthropomorphic prosthetic hands,” in *IEEE International Conference on Rehabilitation Robotics (ICORR)*, 29 2011-july 1 2011, pp. 1–7.
- [7] T. Feix, “Anthropomorphic hand optimization based on a latent space analysis.” PhD Thesis, Vienna University of Technology, 2011.
- [8] T. Feix, J. Romero, C. Ek, H. Schmedmayer, and D. Kragic, “A metric for comparing the anthropomorphic motion capability of artificial hands,” *IEEE Transactions on Robotics*, vol. 29, no. 1, pp. 82–93, Feb 2013.
- [9] L.-C. Kuo, H.-Y. Chiu, C.-W. Chang, H.-Y. Hsu, and Y.-N. Sun, “Functional workspace for precision manipulation between thumb and fingers in normal hands,” *Journal of electromyography and kinesiology*, vol. 19, no. 5, pp. 829–839, oct 2009.
- [10] M. V. Liarokapis, P. K. Artemiadis, and K. J. Kyriakopoulos, “Quantifying anthropomorphism of robot hands,” in *IEEE International Conference on Robotics and Automation (ICRA)*, 2013, pp. 2041–2046.

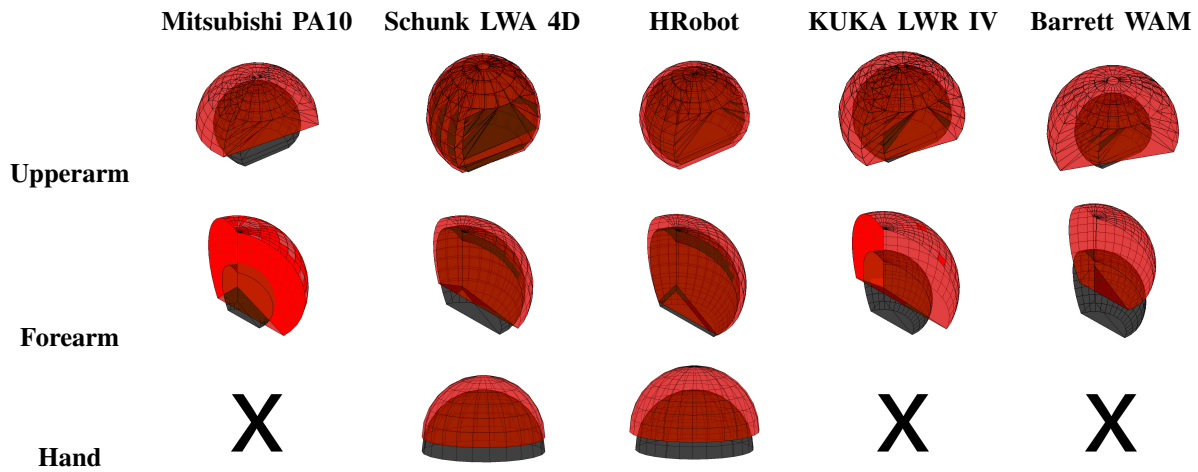


Fig. 3. Links workspaces comparisons between human (black convex hulls) and all robot arms models (red convex hulls), for the case of the actual link lengths. The capital X, denotes those cases for which no intersection between the human and robot link workspaces existed. Thus, for these later cases the score of anthropomorphism is zero.

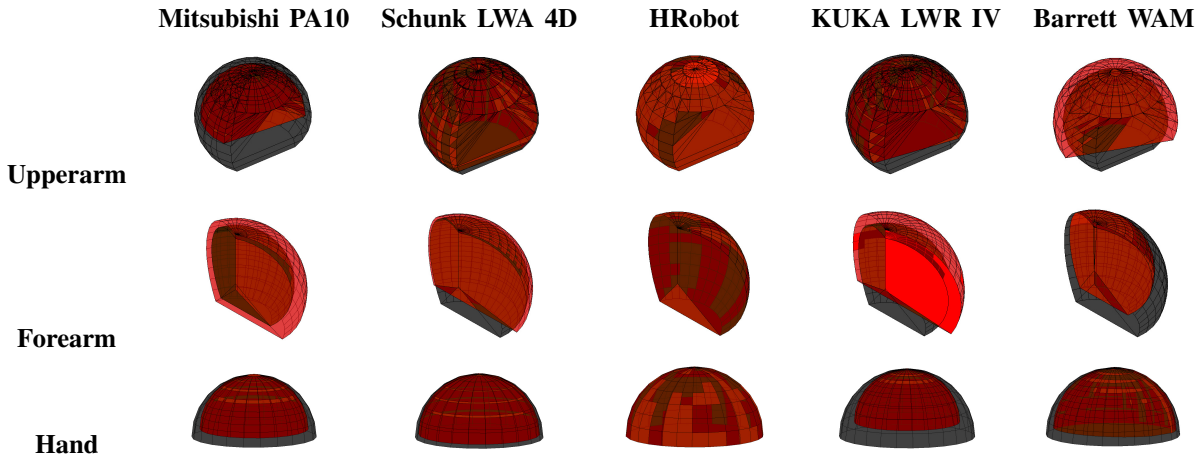


Fig. 4. Links workspaces comparisons between human (black convex hulls) and all robot arms models (red convex hulls), for the case of the normalized link lengths.

[11] F. Zacharias, C. Borst, and G. Hirzinger, "Capturing robot workspace structure: representing robot capabilities," in *IEEE/RSJ International Conference on Intelligent Robots and Systems (IROS)*, nov. 2 2007, pp. 3229–3236.

[12] F. Zacharias, I. S. Howard, T. Hulin, and G. Hirzinger, "Workspace comparisons of setup configurations for human-robot interaction," in *IEEE/RSJ International Conference on Intelligent Robots and Systems (IROS)*. IEEE, 2010, pp. 3117–3122.

[13] J. J. Craig, *Introduction to Robotics: Mechanics and Control*, 3rd ed. Prentice Hall, 2004.

[14] M. A. McDowell, C. D. Fryar, C. L. Ogden, and K. M. Flegal, "Anthropometric reference data for children and adults: United States, 2003-2006." Tech. Rep., 2008.

[15] D. A. Winter, *Biomechanics and Motor Control of Human Movement*. John Wiley & Sons, Inc., 2009.

[16] P. K. Artemiadis, P. T. Katsiaris, M. V. Liarokapis, and K. J. Kyriakopoulos, "On the effect of human arm manipulability in 3d force tasks: Towards force-controlled exoskeletons," in *IEEE International Conference on Robotics and Automation (ICRA)*, May 2011, pp. 3784–3789.

[17] E. Churchill, L. L. Laubach, J. T. Mcconville, and I. Tebbets, "Anthropometric source book. Volume 1: Anthropometry for designers," *Man/System Technology and Life Support*, 1978.

[18] N. Bompos, P. Artemiadis, A. Oikonomopoulos, and K. Kyriakopoulos, "Modeling, full identification and control of the mitsubishi pa-10 robot arm," in *IEEE/ASME international conference on Advanced Intelligent Mechatronics*, Sept., pp. 1–6.

[19] Barrett, "WAM Robot Arm," [Online; accessed 15-March-2013]. [Online]. Available: <http://www.barrett.com/robot/products-arm.htm>

[20] KUKA, "LWR 4 Robot Arm," [Online; accessed 15-March-2013]. [Online]. Available: <http://www.intermodalics.eu/robots/lwr-4>

[21] Schunk, "LWA 4 Robot Arm," [Online; accessed 15-March-2013]. [Online]. Available: <http://mobile.schunk-microsite.com/en/produkte/produkte/dextrous-lightweight-arm-lwa-4d.html>

[22] C. B. Barber, D. P. Dobkin, and H. Huhdanpaa, "The quickhull algorithm for convex hulls," *ACM Transactions on Mathematical Software*, vol. 22, no. 4, pp. 469–483, 1996.

[23] J. Lawrence, "Polytope volume computation," *Mathematics of Computation*, vol. 57, no. 195, pp. 259–271, July 1991.

[24] A. Enge and K. Fukuda, "Exact volume computation for polytopes: a practical study," in *in: Polytopes combinatorics and computation (Oberwolfach)*, 1997, pp. 131–154.

[25] M. Kvasnica, P. Grieder, and M. Baotić, "Multi-Parametric Toolbox (MPT)," 2004. [Online]. Available: <http://control.ee.ethz.ch/~mpt/>

[26] P. Corke, "MATLAB toolboxes: robotics and vision for students and teachers," *IEEE Robotics Automation Magazine*, vol. 14, no. 4, pp. 16–17, dec 2007.